PERGAMON

International Journal of Solids and Structures 40 (2003) 5621–5634

INTERNATIONAL JOURNAL OF SOLIDS and STRUCTURES

www.elsevier.com/locate/ijsolstr

The use of graded finite elements in the study of elastic wave propagation in continuously nonhomogeneous materials

Michael H. Santare [a,*], Priya Thamburaj [a,*], George A. Gazonas [b]

[a] *Department of Mechanical Engineering and Center for Composite Materials, University of Delaware, Newark, DE 19716, USA*
[b] *Weapons and Materials Research Directorate, US Army Research Laboratory, Aberdeen Proving Ground, MD 21005, USA*

Received 16 May 2003; received in revised form 28 May 2003

Abstract

Finite elements with graded properties are used to simulate elastic wave propagation in functionally graded materials. The graded elements are formulated with continuously nonhomogeneous material property fields and compared to conventionally formulated homogeneous elements. An example problem is solved for the two-dimensional case to show the potential benefits of the graded formulation. It is observed that the conventional elements give a discontinuous stress field in the direction perpendicular to the material property gradient, while the graded elements give a continuous distribution. In the one-dimensional case, the solutions are compared to the analytical solutions by Chiu and Erdogan [J. Sound Vib. 222 (3) (1999) 453]. The results show that for identical levels of mesh refinement, the graded formulation produces similar spatial resolution, and temporal resolution for the range of boundary value problems studied. Observations are explained and their implications for numerical modeling are discussed.

Keywords: Elastic wave propagation; Functionally graded materials; Graded finite elements

1. Introduction

Many naturally occurring material systems have mechanical properties that vary continuously as a function of position. These systems can be described as continuously nonhomogeneous materials. Examples of this type of material are animal tissues (e.g. bone, cartilage), plant structures (e.g. wood, cellulose etc.) and geological materials (e.g. rocks, soil). The mechanical benefits obtained from such a material gradient may be significant, as can be seen by the excellent structural performance of some of these natural materials. Consequently, there has been increasing interest in producing man-made continuously nonhomogeneous materials for specific applications, often referred to as functionally graded materials (FGMs). However, numerous obstacles to the widespread use of FGMs remain, not only because of the difficulty in

* Corresponding authors. Tel.: +1-302-8310379; fax: +1-302-8313619.
E-mail address: thambura@ccm.udel.edu (P. Thamburaj).

0020-7683/$ - see front matter
doi:10.1016/S0020-7683(03)00315-9

manufacturing such materials, but also because of a lack of fundamental understanding of their mechanical response relative to homogeneous or even composite material systems. Accurate and efficient numerical methods can go a long way to help bridge this gap in understanding.

Conventional finite element formulations assign a single set of material properties to each element such that the property field is constant within an individual element. To model a continuously nonhomogeneous material this way, one must discretize the material property functions at the size scale of the element mesh, producing a step-wise constant approximation to the property field. If the property gradient follows the same contours as the geometry, the element rows can be aligned with the gradient direction and each row of homogeneous elements assigned the material properties for the midline of the row. This is a relatively simple and effective approximation. If however, the material property gradient is not aligned with the domain geometry, this approximation can produce an awkward model with significant artificial discontinuities. This is shown schematically in Fig. 1. The left-hand drawing shows a radial mesh with a vertical continuous property gradient (grey-scale) superimposed. When the centroidal material property (grey-scale) is assigned to each finite element, the resulting mesh is shown in the right-hand drawing.

This step-wise constant approximation to continuous material properties has been used in much of the literature involving numerical simulations of functionally graded materials (Li et al., 2000; Marur and Tippur, 2000; Anlas et al., 2000; Li et al., 2001). Some of this previous work (Anlas et al., 2000), specifically shows that this piece-wise constant approximation can be used to provide fairly accurate global energy calculations and that only the local stresses and displacements within each element are affected. However, in some engineering applications, such as failure analysis, crack growth or stress wave propagation, these local values may be of critical importance.

Recently, Banks-Sills et al. (2002) looked at the effects of using different types of finite element approximations on the predicted stress wave propagation through a graded material. They simulated one-dimensional stress waves traveling through a graded composite material using a distinct phase model, a discretely layered model and a smoothly varying model. Although conventional elements were used in the study, they showed that different levels of discretization caused a relative shift in the speed of the wave and that the magnitude of the shift increases as time increases.

Scheidler and Gazonas (2002) studied unidirectional wave propagation in an elastic media with a quadratic impedance variation through the thickness, subjected to both an applied step in stress and impact loading. They compared solutions generated using a discretely layered DYNA3D model with hexahedral elements to analytical solutions. For the applied step in stress loading, increasing mesh density from 30 to 300 elements through the thickness improved solution accuracy, but both the compressive and tensile stress wave amplitudes were underestimated, particularly at later times. For the impact loading case, however DYNA3D did a much better job at modeling the analytical response.

In separate studies, Santare and Lambros (2000) and Kim and Paulino (2002b) showed that graded finite elements have the potential to provide improved accuracy without increasing the number of degrees of freedom for a given model. In these studies, both sets of investigators looked at two-dimensional static

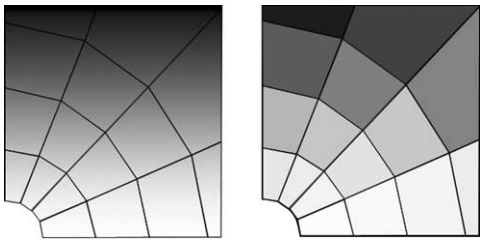

Fig. 1. Schematic showing the effect of using uniform conventional finite elements to model a continuously graded medium.

elasticity boundary value problems using slightly different graded element formulations. The results showed that for identical meshes, with equal degrees of freedom, the graded element formulations outperform conventional, homogeneous elements when the loading is perpendicular to the gradient direction. Although the average stresses for the individual elements were nearly identical, the local values (on the sub-element size scale) were far closer to the analytical values in the graded formulation. In addition, the stress distribution across element borders was more nearly continuous, as would be the case in an actual system. In other words, there was less of an artificial "jump" in stress from element to element with the graded formulation. However, when the loading is parallel to the gradient direction, the graded four-node isoparametric formulation predicts sharp jumps in stress at the element borders while the conventional formulation does not. Kim and Paulino (2002b) show that this problem can be reduced or eliminated by the use of higher-order isoparametric elements. In the work presented here, we extend the previous, graded finite element formulation of Santare and Lambros (2000) to study elastic stress waves in continuously nonhomogeneous materials.

The use of a graded finite element has several potential advantages over the use of conventional elements in the study of elastic stress waves. In the general case, the property gradient in a continuously nonhomogeneous material will cause a continuous variation in the acoustic impedance as a function of position. In a conventional finite element model of a continuously nonhomogeneous material, the model produces a piece-wise constant approximation for the actual impedance. This will cause discrete boundaries for the stress waves where in the actual continuously nonhomogeneous system these distinct boundaries would not exist. These boundaries have a cumulative effect on the magnitude and speed of propagating stress waves (Lee et al., 1975).

As an additional consideration, as in the static case, greater accuracy may be obtained on the local scale without additional refinement of the mesh. This advantage may be particularly important in an explicit dynamic finite element implementation. In such a formulation, the dimensions of the elements govern the length of the time increment that can be used in the solution. Essentially, the time step must be smaller than the time it takes for a stress wave to travel across the element, this is commonly referred to as the Courant condition. If this condition is met, the time integration will converge; if not, the solution will become unstable. Therefore, an element that increases the local accuracy of the calculations, without decreasing the element dimensions could have a positive impact on the performance of an explicit-dynamic finite element code.

2. Formulation of the stiffness matrix

In the present study, all finite element results are generated using a displacement based, updated-Lagrangian code with explicit time integration. It uses artificial viscosity to provide shock capture and suppress Gibb's phenomenon. The code was developed in-house as a platform for testing the mathematical formulations that follow. For a given mesh, using conventional elements, the code produces results nearly identical to commercial codes for small-displacement, elastic wave propagation.

In the standard formulation of the stiffness matrix for a conventional isoparametric finite element, one starts with an assumed set of interpolation functions such that the displacement in the element can be written (see for example: Bathe and Wilson, 1976)

$$u(x) = \sum_{I=1}^{n} N_I(x) U_I. \tag{1}$$

Here $u(x)$ is a matrix of the displacement components (each a function of position within the element), $N_I(x)$ is the matrix of interpolation or shape functions and U_I are the nodal displacement values for each of the "n" nodes of the element. To find the infinitesimal strain components, $\varepsilon(x)$ one can write,

$$\varepsilon(x) = \sum_{I=1}^{n} B_I(x) U_I, \tag{2}$$

where $B_I(x)$ is the matrix of the appropriate spatial derivatives of the shape functions $N_I(x)$. In large deformation problems, this same expression can be used to find the strain increment due to a displacement increment.

Assuming linear elastic material behavior, the stress increment components at a point $\sigma(x)$ are calculated from the strain increment at that point through the material property matrix $C(x)$ such that,

$$\sigma(x) = C(x)\varepsilon(x). \tag{3}$$

Traditionally, the components of the $C(x)$ matrix are chosen to be constant material properties for each finite element. However, there is no fundamental reason that these elastic properties cannot be spatially variable functions within an element. In the case of a graded material, the components of $C(x)$ could be explicit functions describing the actual material property gradients. In any case, we define the element stiffness matrix K^{e} as the linear function that maps the nodal displacements U_I to the nodal forces f_I for the element

$$f_I = K^{\mathrm{e}} U_I. \tag{4}$$

By applying the principle of virtual work, the work done by the nodal forces must be equal to the work of deformation within the element. Setting these two quantities equal we can derive the following expression for the element stiffness matrix

$$K^{\mathrm{e}} = \int_{V_{\mathrm{e}}} B^{\mathrm{T}}(x) C(x) B(x)\, \mathrm{d}V, \tag{5}$$

where the integral is taken over the volume of the element V_{e}. This is certainly not the only way one can choose to formulate graded finite elements, but it is probably the most straightforward way. This direct approach has been used in several previous studies (Gu et al., 1999; Santare and Lambros, 2000; Kim and Paulino, 2002a) and shown to provide an improvement in accuracy for static two-dimensional boundary value problems. In the present study, we extend this approach to include the dynamic response of elastic materials.

Up to this point, the only numerical approximation used in the formulation was the imposition of the interpolation functions in Eq. (1). On the element level, the accuracy of this numerical approximation is dependent on the compatibility of the assumed shape functions $N_I(x)$ to the exact displacement field. (Exact here refers to the analytical solution of the field equations under the assumptions of linear elastic response and infinitesimal strain.) In fact, if a set of shape functions is chosen which is perfectly compatible with the exact displacement solution, the finite element results will capture this solution with any level of mesh refinement. For example, a bilinear displacement field will be accurately predicted by one or more elements employing bilinear interpolation functions.

3. Formulation of the mass matrix

For a functionally graded elastic material, the mass density will, in general, be a function of position as well as the material moduli. Therefore, in the most general graded element, the mass density distribution should be incorporated into the element formulation in the same manner as the material moduli. However, in terms of developing the mass matrix, there is an additional complication; there are several, commonly accepted methods for formulating the mass matrix for an isoparametric element. The consistent mass matrix approach follows the same basic procedure as outlined above for the stiffness. Namely, the inter-

polation functions, multiplied by the mass density function $\rho(x)$, are integrated over the element volume to find the element mass matrix, M^e

$$M^e = \int_{V_e} N^T(x) N(x) \rho(x) \, dV. \tag{6}$$

The other commonly used formulation is the lumped mass matrix. In this approach, the mass of the element is assumed to be concentrated at the element nodes. Each node therefore is assigned a portion of the total element mass and the resulting mass matrix is a diagonal matrix. The determinant of the Jacobian matrix, evaluated at a specific node location corresponds to the portion of the total element volume associated with that node. In the conventional finite element approach, this volume is simply multiplied by the constant mass density of the element to determine the value of the lumped mass at the node. A major advantage of the lumped mass approach is that the resulting matrix is diagonal and therefore the numerical inversion requires far less computation than the inversion of a fully populated matrix.

Using either approach, a graded form of the mass matrix can be developed. In the case of the consistent mass matrix, one needs to input the proper density distribution $\rho(x)$ into Eq. (6) and integrate. The result is a fully populated mass matrix that incorporates the nonhomogeneous density distribution. In the case of the lumped mass approach, one needs to assign a density value to each sub-volume within the element. (An obvious choice is the mass density at the centroid of the sub-volume.) The resulting nodal masses must then be scaled to ensure that the total mass of the element is conserved. The result of this calculation is then a diagonal, lumped mass matrix that approximates the nonhomogeneous mass distribution. The finite elements in the following examples are formulated with a graded stiffness or a graded density and in both cases the formulation used is a consistent mass matrix approach.

4. Analytical solutions

Chiu and Erdogan (1999) present exact, one-dimensional solutions for a rectangular pressure pulse loading on the $x = l$ face of an infinite slab ($0 \leqslant x \leqslant l$) and subject to either free–free or fixed–free end conditions. These solutions were chosen for comparison to the finite element results in this study because they are among the few analytical solutions available for nonhomogeneous materials where the stiffness and density can be varied independently of one another. This means that the wave speed can also be a function of position. The exact one-dimensional results presented by Chiu and Erdogan are the solutions to the differential equation

$$\frac{d}{dx}\left(E(x)\frac{d}{dx}u(x,t)\right) = \rho(x)\frac{d^2}{dt^2}u(x,t) \tag{7}$$

with the following material property functions

$$E(x) = E_0\left(a\frac{x}{l} + 1\right)^m, \tag{8}$$

$$\rho(x) = \rho_0\left(a\frac{x}{l} + 1\right)^n. \tag{9}$$

In Eqs. (7)–(9) $u(x,t)$ is the displacement, $E(x)$ and $\rho(x)$ are the modulus and density and E_0, ρ_0, a, m, n are material constants ($a > -1$) that describe the property gradients.

5. Results

As a means of comparison, identical meshes of graded finite elements and conventional finite elements are used to solve identical boundary value problems. Ideally, we would like to compare all the numerical solutions to exact analytical solutions to determine the relative merit of the two methods. This is done in the following, for a series of one-dimensional problems solved analytically by Chiu and Erdogan (1999). However, the authors have not found suitable two or three-dimensional analytical solutions for comparison. Therefore, graded and conventional finite element results are simply compared to each other for an example two-dimensional problem. The domain and property gradient for this example problem are chosen to coincide with those of the exact analytical one-dimensional solutions.

The two-dimensional example problem, shown in Fig. 2a, consists of a square domain with a material property gradient in the x direction. For this example, we choose a second order variation in elastic modulus and a constant mass density. The modulus variation is defined by Eq. (8) with $E_0 = 3 \times 10^8$ psi, $m = 2$ and $a = -0.9$. The constant density is defined by Eq. (9) with $\rho_0 = 7.33 \times 10^{-3}$ $\mathrm{lb_f\,s^2/in.^4}$ and $n = 0$. This corresponds to a modulus that goes from $E = 3 \times 10^8$ psi at $x = 0$ to $E = 3 \times 10^6$ psi at $x = l$ (decreasing stiffness). The loading is a 1000 lb square-wave point impulse of 50 μs duration on the top surface at $x = l/2$, $y = l$. We solve the problem with conventional finite elements and with the graded elements described in this paper. In both cases, the mesh consists of 20×20 four-node isoparametric elements. Fig. 3 shows the σ_y stress near the center of the domain $y = l/2$ for three consecutive time steps, 7.5, 8.5 and 9.5 μs. The graph shows the σ_y stress calculated at specific points within the element and the results are not interpolated from element to element. The conventional finite element solution is labeled FEM, and the graded formulation is labeled FEMg. Fig. 4 shows σ_y near the bottom of the domain $y = 0$ at, 15, 16 and 17 μs. These positions and times were chosen to show the arrival of the first wave front so that the complicating effects of reflections do not obscure the results.

In the next series of figures, we compare a standard, eight-node, isoparametric finite element solution, and a solution using the eight-node graded element formulation, to the analytical solutions of Chiu and Erdogan (1999). Our choice of specific boundary value problem is dictated by the form of the exact analytical solutions used as the standard for comparison (Eqs. (7)–(9)). As a first one-dimensional example, we choose the same domain and properties as used in the two-dimensional example. In all these one-dimensional cases, the domain is loaded at $x = l$ by a 1000 psi, rectangular pressure pulse of 50 μs duration and the other end at $x = 0$ is fixed with zero displacement (see Fig. 2b).

Figs. 5–8 show the longitudinal stress for this first, one-dimensional example, near the center of the domain $x = l/2$ as a function of time. Each figure gives the same longitudinal stress component as calculated from progressively finer finite element meshes and compares to the analytical solution from Chiu and Erdogan. For the conventional finite element formulation, the modulus at each element centroid was used as the element stiffness. For the graded formulation, the local modulus at each integration point,

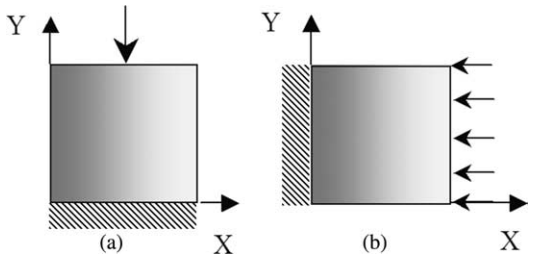

Fig. 2. Boundary value problems considered. (a) 2-D domain fixed at $y = 0$ point load at $y = l$, (b) 1-D domain fixed at $x = 0$, uniform load at $x = l$.

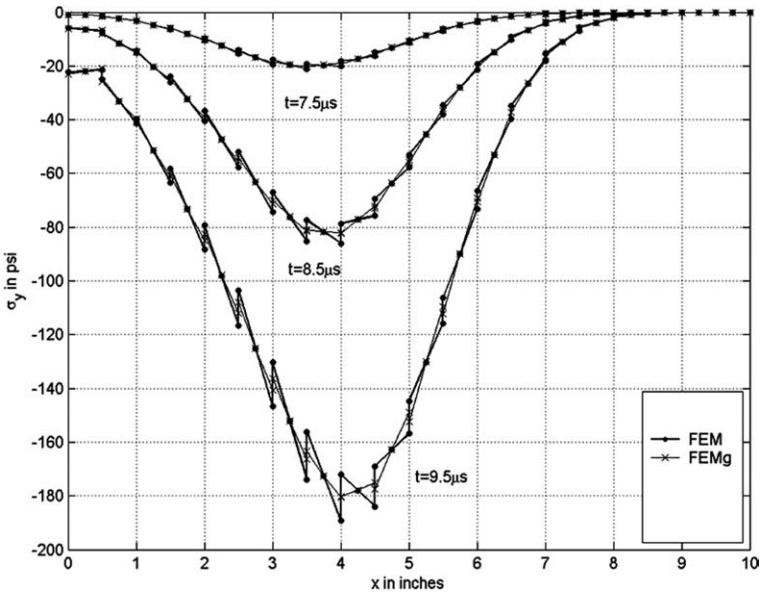

Fig. 3. Longitudinal stress vs X at $y = 5.125$ for $a = -0.9$, $m = 2$ and $n = 0$ in Eqs. (8) and (9) with free–fixed boundary conditions, 2-D FEM model with 20×20 elements.

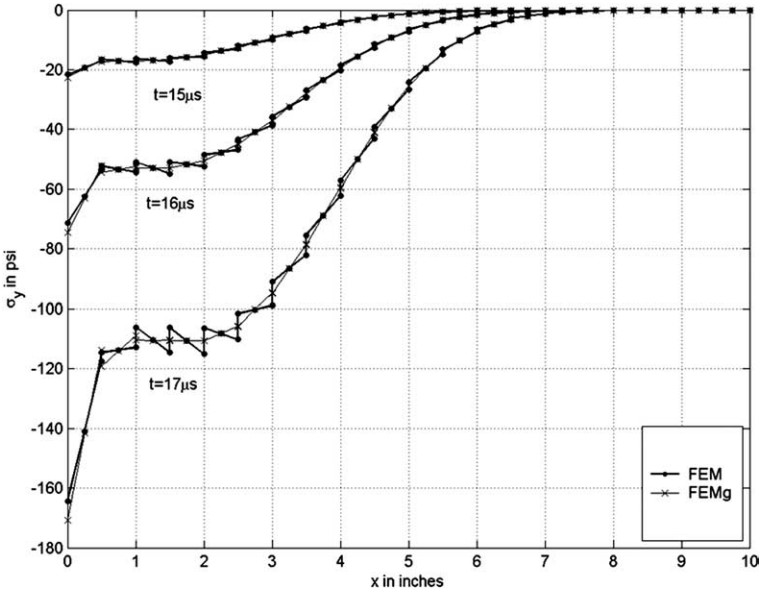

Fig. 4. Longitudinal stress vs X at $y = 0.125$ for $a = -0.9$, $m = 2$ and $n = 0$ in Eqs. (8) and (9) with free–fixed boundary conditions, 2-D FEM model with 20×20 elements.

calculated using Eq. (8), was used. Again, the graphs show the stress calculated at a specific point within the element and results are not interpolated from element to element.

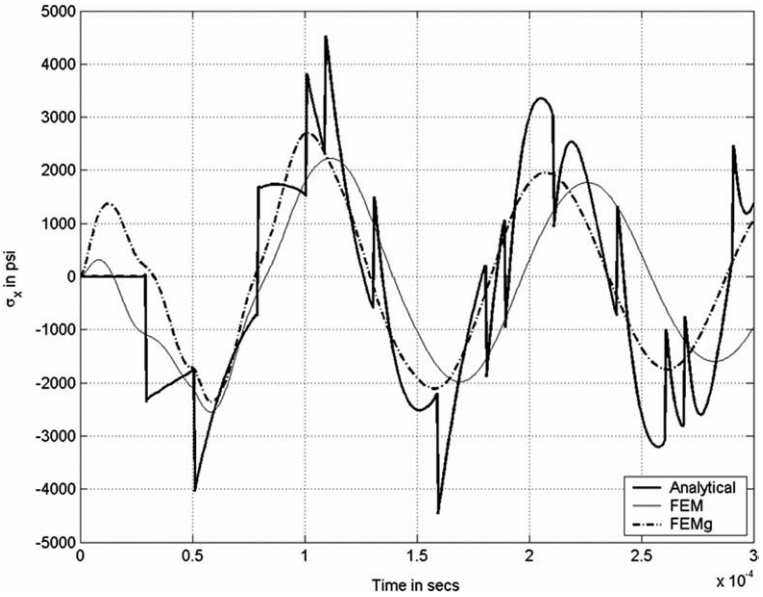

Fig. 5. Longitudinal stress vs time at $x = 5.125$ for $a = -0.9$, $m = 2$ and $n = 0$ in Eqs. (8) and (9) with free–fixed boundary conditions, FEM models with two elements.

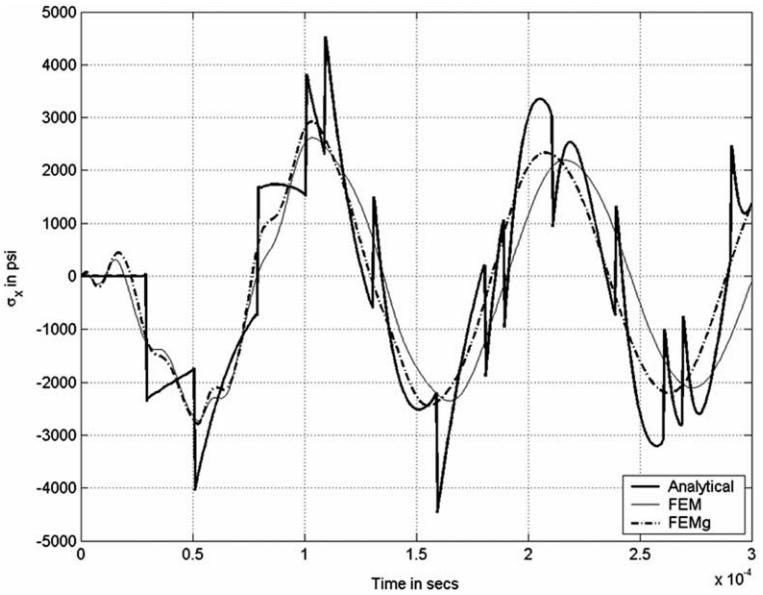

Fig. 6. Longitudinal stress vs time at $x = 5.125$ for $a = -0.9$, $m = 2$ and $n = 0$ in Eqs. (8) and (9) with free–fixed boundary conditions, FEM models with four elements.

In the second one-dimensional example, we again use the same domain but with a second order variation in mass density and a constant elastic modulus. The density variation is defined by Eq. (9) with $\rho_0 = 0.0733$ $lb_f\ s^2/in.^4$, $n = -2$ and $a = 9$. The constant elastic modulus is defined by Eq. (8) with $E_0 = 120 \times 10^6$ psi and

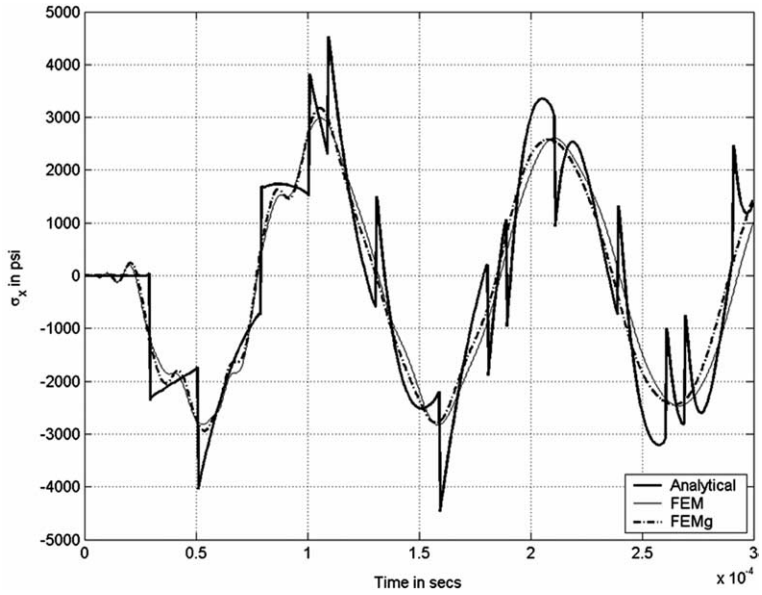

Fig. 7. Longitudinal stress vs time at $x = 5.125$ for $a = -0.9$, $m = 2$ and $n = 0$ in Eqs. (8) and (9) with free–fixed boundary conditions, FEM models with eight elements.

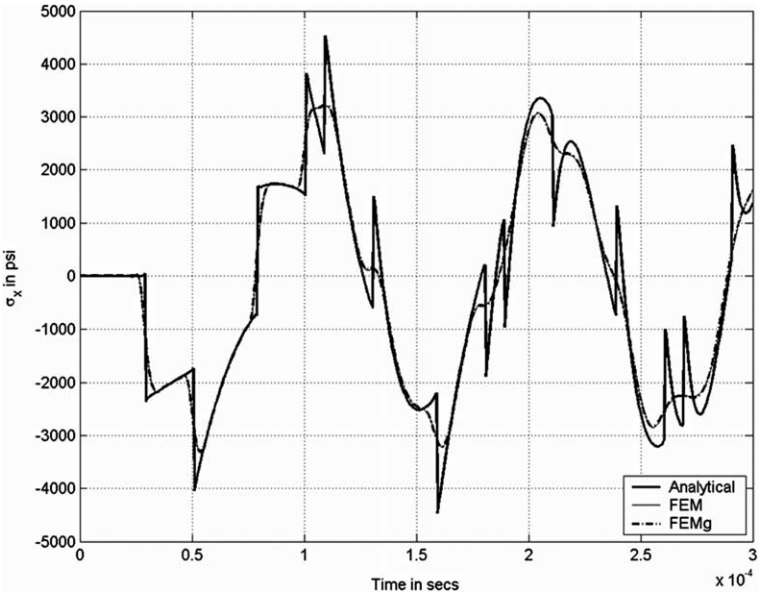

Fig. 8. Longitudinal stress vs time at $x = 5.125$ for $a = -0.9$, $m = 2$ and $n = 0$ in Eqs. (8) and (9) with free–fixed boundary conditions, FEM models with 40 elements.

$m = 0$. This corresponds to a density that goes from $\rho = 0.0733\ \mathrm{lb_f\ s^2/in.^4}$ at $x = 0$ to $\rho = 0.000733\ \mathrm{lb_f\ s^2/in.^4}$ at $x = l$ (decreasing density). As in the previous example, the domain is loaded at $x = l$ by a 1000 psi, rectangular pressure pulse of 50 μs duration and the other end at $x = 0$ is fixed with zero displacement.

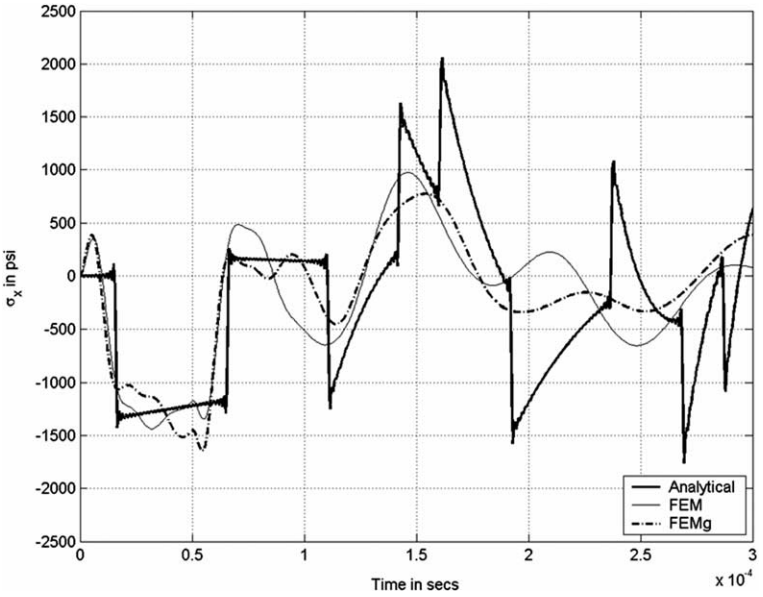

Fig. 9. Longitudinal stress vs time at $x = 5.125$ for $a = 9$, $m = 0$ and $n = -2$ in Eqs. (8) and (9) with free–fixed boundary conditions, FEM models with two elements.

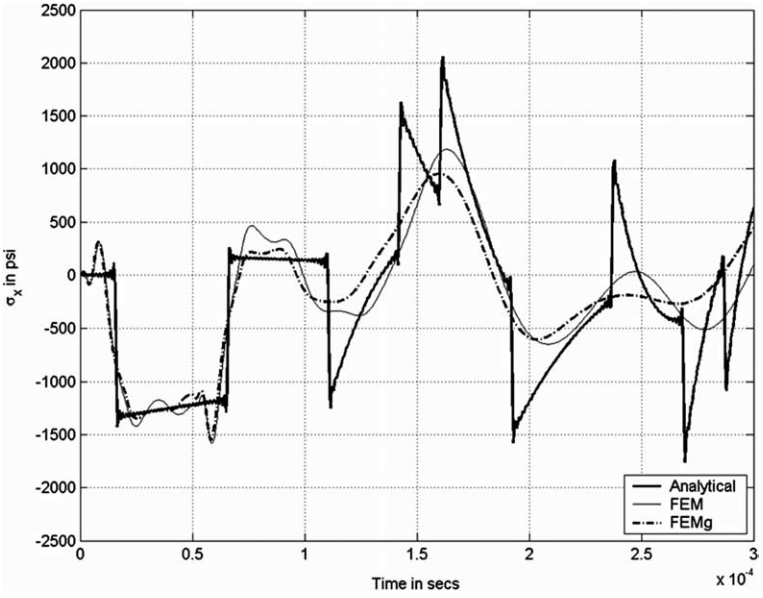

Fig. 10. Longitudinal stress vs time at $x = 5.125$ for $a = 9$, $m = 0$ and $n = -2$ in Eqs. (8) and (9) with free–fixed boundary conditions, FEM models with four elements.

Figs. 9–12 again show the longitudinal stress near the center of the domain $x = l/2$ as a function of time. Each figure gives the same longitudinal stress component as calculated from progressively finer finite element meshes and compares to the analytical solution from Chiu and Erdogan. For the conventional finite element

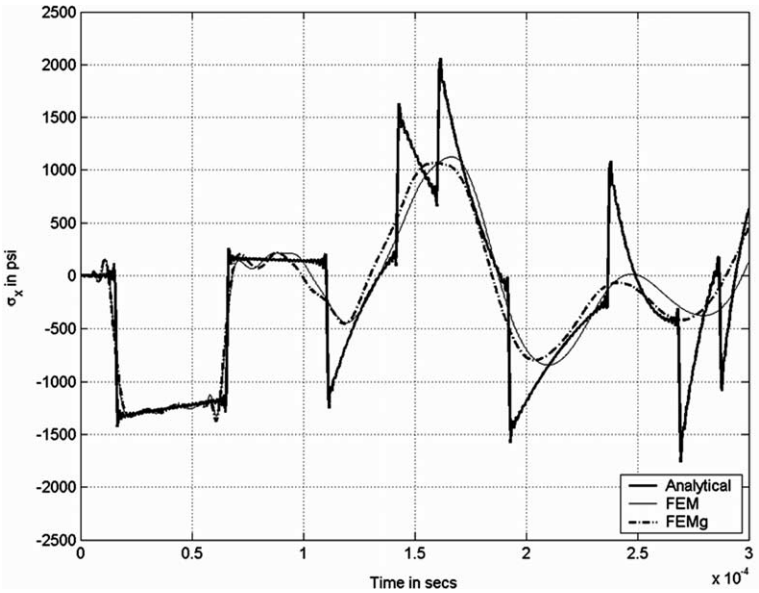

Fig. 11. Longitudinal stress vs time at $x = 5.125$ for $a = 9$, $m = 0$ and $n = -2$ in Eqs. (8) and (9) with free–fixed boundary conditions, FEM models with eight elements.

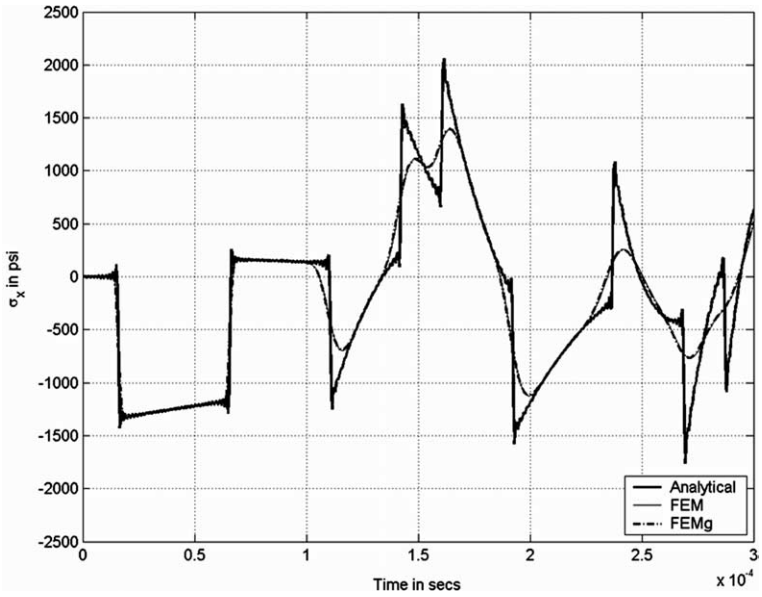

Fig. 12. Longitudinal stress vs time at $x = 5.125$ for $a = 9$, $m = 0$ and $n = -2$ in Eqs. (8) and (9) with free–fixed boundary conditions, FEM models with 40 elements.

formulation, the density at each element centroid was used as the element density. For the graded formulation, the local density at each integration point, calculated using Eq. (9), was used. As in the previous figures, the conventional finite element solution is labeled FEM, and the graded formulation is labeled FEMg.

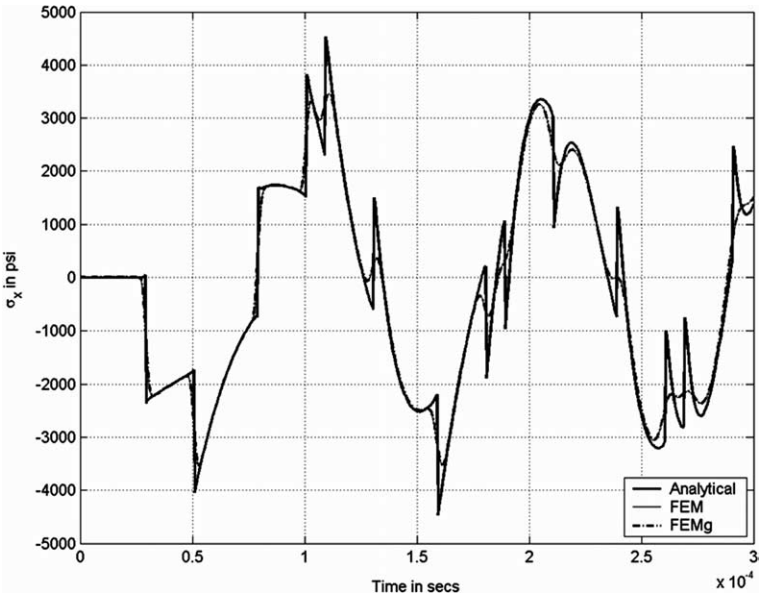

Fig. 13. Longitudinal stress vs time at $x = 5.125$ for $a = -0.9$, $m = 2$ and $n = 0$ in Eqs. (8) and (9) with free–fixed boundary conditions, FEM models with 100 elements.

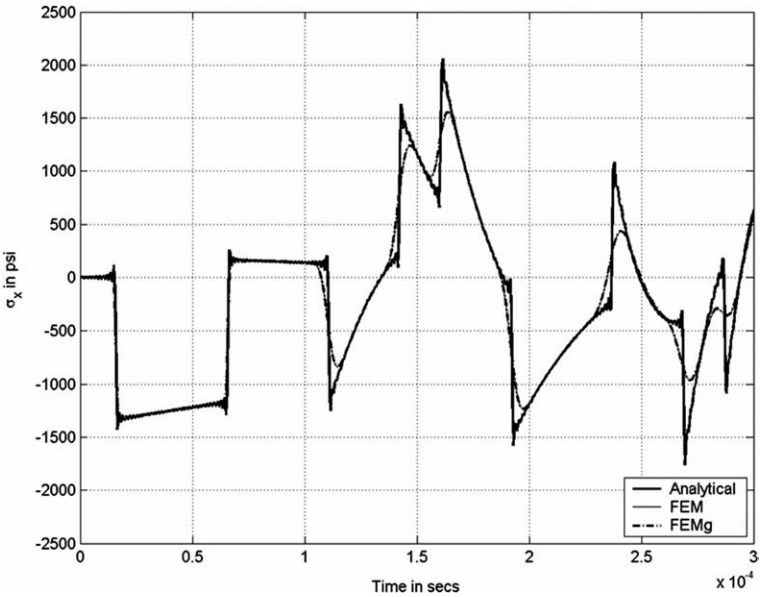

Fig. 14. Longitudinal stress vs time at $x = 5.125$ for $a = 9$, $m = 0$ and $n = -2$ in Eqs. (8) and (9) with free–fixed boundary conditions, FEM models with 100 elements.

In order to show that both formulations eventually converge to the exact solution, results from more highly refined meshes are shown in Figs. 13 and 14. These plots show the 100 element solutions for the same boundary value problems shown in Figs. 5–12.

6. Discussion and conclusions

For the two-dimensional example problem shown in Figs. 2a, 3 and 4, no analytical solution is provided for comparison. Therefore, we cannot comment on the accuracy of the graded elements relative to the conventional formulation. What is apparent however, is that at the level of mesh refinement shown, the two solutions present significantly different stresses at the local, sub-element size scale. The conventional elements give a discontinuous stress field in the direction perpendicular to the material property gradient, while the graded elements give a continuous distribution. Recall that the graphs show the stress calculated at specific points within the element and the results are not interpolated from element to element. The stress values at the centroids of the elements coincide, but the stresses computed at other points within the element differ since these values depend on the curvature of the stress fronts. This phenomenon is precisely the same as that seen in the two-dimensional static elastic formulation in the recent literature. For a thorough explanation of this effect, please refer to Santare and Lambros (2000). It is observed that this trend persists at later times, however due to reflections from the boundaries, the stress fronts then become complicated and are difficult to discern. Alternatively, the stress vs time history at a particular point follows a trend similar to the one-dimensional case shown in Figs. 5–8. Since these graphs do not convey any additional information for the two-dimensional case, they have not been included in this paper.

Referring to the one-dimensional results, at the lower levels of mesh refinement, neither finite element formulation can capture the sharp peaks in the analytical curves. In fact, in both sets of FEM solutions there is a gradual reduction in relative peak stress with increasing time. This reduction is due to the artificial damping included in the finite element program to reduce the effects of noise and prevent element collapse in compression. The change in amplitude for both FEM solutions relative to the analytical solution is strongly dependent on the particular value chosen for the artificial damping used in the FEM code. In other words, a small change in this parameter will result in a significant change in wave amplitude at large times. However, another phenomenon can be seen in these figures. The conventional FEM results are ''slowing down'' relative to the analytical solution, while the FEMg graded solution is tracking the analytical solution more closely. This phenomenon is more apparent at later times and with coarser meshes. In the coarsest mesh considered, the lag between the FEM and FEMg solutions is approximately 10% of the solution time. At higher mesh refinement, both formulations give significantly better results, as seen in Fig. 13 for example but one can conclude that at even later times, these solutions will diverge as well. This is hard to show however due to the effects of the artificial damping described above.

An eight-node isoparametric formulation was used to solve the one-dimensional examples presented in this work. Previous studies of graded finite elements (Santare and Lambros, 2000; Kim and Paulino, 2002b) have identified certain inaccuracies associated with a four-node formulation in one-dimensional static problems. As explained in Kim and Paulino (2002b) using an eight-node formulation can eliminate these inaccuracies. Preliminary results from the present study indicated that the same behavior occurs in the dynamic case as well. In order to compare the two finite element approaches on an equal basis, identical meshes with the same nodes and degrees of freedom are used in each figure. This means that the element dimensions, their critical time steps and the actual CPU run-times for the conventional and graded formulations are nearly identical at each level of mesh refinement.

In many cases, it may be sufficient to use mesh refinement to obtain better local stress values without the complication of the graded element formulation. However, in problems involving continuously nonhomogeneous materials, the graded element has some potential. As the preceding results show, in one-dimensional wave problems, the more complicated formulation may be justified for solving some problems. Further work is needed to fully explore the potential of using the graded element formulation in dynamic boundary value problems, especially in two and three-dimensional wave propagation problems.

Acknowledgement

The authors wish to acknowledge support of this research from the Composite Materials Technology Grant awarded to the Center for Composite Materials from the United States Army Research Laboratory.

References

Anlas, G., Santare, M.H., Lambros, J., 2000. Numerical calculation of stress intensity factors in functionally graded materials. International Journal of Fracture 104 (2), 131–143.

Banks-Sills, L., Eliasi, R., Berlin, Y., 2002. Modeling of functionally graded materials in dynamic analyses. Composites: Part B 33, 7–15.

Bathe, K.-J, Wilson, E.L., 1976. Numerical Methods in Finite Element Analysis. Prentice Hall, Englewood Cliffs, NJ.

Chiu, T.-C., Erdogan, F., 1999. One-dimensional wave propagation in a functionally graded elastic medium. Journal of Sound and Vibration 222 (3), 453–487.

Gu, P., Dao, M., Asaro, R.J., 1999. A simplified method for calculating the crack tip field of functionally graded materials using the domain integral. Journal of Applied Mechanics 66, 101–108.

Kim, J.H., Paulino, G.H., 2002a. Finite element evaluation of mixed-mode stress intensity factors in functionally graded materials. International Journal for Numerical Methods in Engineering 53, 1903–1935.

Kim, J.H., Paulino, G.H., 2002b. Isoparametric graded finite elements for nonhomogeneous isotropic and orthotropic materials. Journal of Applied Mechanics 69 (2), 502–514.

Lee, E.H., Budiansky, B., Drucker, D.C., 1975. On the influence of variations of material properties on stress wave propagation through elastic slabs. Journal of Applied Mechanics 42 (2), 417–422.

Li, H., Lambros, J., Cheeseman, B.A., Santare, M.H., 2000. Experimental investigation of the quasi-static fracture of functionally graded materials. International Journal of Solids and Structures 37 (27), 3715–3732.

Li, Y., Ramesh, K.T., Chin, E.S.C., 2001. Dynamic characterization of layered and graded structures under impulsive loading. International Journal of Solids and Structures 38, 6045–6061.

Marur, P.R., Tippur, H.V., 2000. Numerical analysis of crack-tip fields in functionally graded materials with a crack normal to the elastic gradient. International Journal of Solids and Structures 37, 5353–5370.

Santare, M.H., Lambros, J., 2000. Use of a graded finite element to model the behavior of nonhomogeneous materials. Journal of Applied Mechanics 67 (4), 819–822.

Scheidler, M.J., Gazonas, G.A., 2002. Analytical and computational study of one-dimensional impact of graded elastic solids. In: Shock Compression of Condensed Matter 2001, Melville, NY, pp. 689–692.